HHS Public Access

Author manuscript

Circulation. Author manuscript; available in PMC 2019 December 04.

Published in final edited form as:

Circulation. 2018 December 04; 138(23): 2666–2681. doi:10.1161/CIRCULATIONAHA.117.032273.

Determining the Pathogenicity of a Genomic Variant of Uncertain Significance Using CRISPR/Cas9 and Human Induced Pluripotent Stem Cells

Ning Ma, PhD[1,2,3,*], **Joe Zhang, MD, PhD**[1,2,3,*], **Ilanit Itzhaki, PhD**[1,2,3,*], **Sophia L. Zhang, BS**[1,2,3], **Haodong Chen, PhD**[1,2,3], **Francois Haddad, MD**[1,2], **Tomoya Kitani, MD, PhD**[1,2,3], **Kitchener D. Wilson, MD, PhD**[1,2,3], **Lei Tian, PhD**[1,2,3], **Rajani Shrestha, MS**[1,2,3], **Haodi Wu, PhD**[1,2,3], **Chi Keung Lam, PhD**[1,2,3], **Nazish Sayed, MD, PhD**[1,2,3], and **Joseph C. Wu, MD, PhD**[1,2,3]

[1]Stanford Cardiovascular Institute, Stanford University School of Medicine, Stanford, CA 94305, USA

[2]Division of Cardiology, Department of Medicine, Stanford University School of Medicine, Stanford, CA 94305, USA

[3]Institute for Stem Cell Biology and Regenerative Medicine, Stanford University School of Medicine, Stanford, CA 94305, USA

Abstract

Background—The progression towards low-cost and rapid next-generation sequencing has uncovered a multitude of variants of unknown significance (VUS) in both patients and asymptomatic “healthy” individuals. A VUS is a rare or novel variant for which disease pathogenicity has not been conclusively demonstrated or excluded, and thus cannot be definitively annotated. VUS therefore pose critical clinical interpretation and risk-assessment challenges, and new methods are urgently needed to better characterize their pathogenicity.

Methods—To address this challenge and showcase the uncertainty surrounding genomic variant interpretation, we recruited a “healthy” asymptomatic individual, lacking cardiac-disease clinical history, carrying a hypertrophic cardiomyopathy (HCM)-associated genetic variant (NM_000258.2:c.170C>A, NP_000249.1:p.Ala57Asp) in the sarcomeric gene *MYL3*, reported by the ClinVar database to be “likely pathogenic”. Human induced pluripotent stem cells (iPSCs) were derived from the heterozygous VUS$MYL3_{(170C>A)}$ carrier, and their genome was edited using CRISPR/Cas9 to generate four isogenic iPSC lines: (1) corrected “healthy” control, (2) homozygous VUS$MYL3_{(170C>A)}$, (3) heterozygous frameshift mutation (fs) $MYL3^{(170C>A/fs)}$, and (4) known heterozygous *MYL3* pathogenic mutation (NM_000258.2:c.170C>G), at the same nucleotide position as VUS$MYL3_{(170C>A)}$), lines. Extensive assays including measurements of

Correspondence: Joseph C. Wu, 265 Campus Drive, G1120B Stanford, CA 94305-5454. joewu@stanford.edu, PH: 650-736-2246; FAX: 650-736-0234, Twitter handle: @StanfordCVI.

*Contributed equally

DISCLOSURES

None

gene expression, sarcomere structure, cell size, contractility, action potentials, and calcium handling were performed on the isogenic iPSC-derived cardiomyocytes (iPSC-CMs).

Results—The heterozygous VUS*MYL3*$_{(170C>A)}$-iPSC-CMs did not show an HCM phenotype at the gene expression, morphology, or functional levels. Furthermore, genome-edited homozygous VUS*MYL3*$_{(170C>A)}$- and frameshift mutation *MYL3*$^{(170C>A/fs)}$-iPSC-CMs lines were also asymptomatic, supporting a benign assessment for this particular *MYL3* variant. Further assessment of the pathogenic nature of a genome-edited isogenic line carrying a known pathogenic *MYL3* mutation, *MYL3*$_{(170C>G)}$, and a carrier-specific iPSC-CMs line, carrying a, *MYBPC3*$_{(961G>A)}$ HCM variant demonstrated the ability of this combined platform to provide both pathogenic and benign assessments.

Conclusions—Our study illustrates the ability of CRISPR/Cas9 genome-editing of carrier-specific iPSCs to elucidate both benign and pathogenic HCM functional phenotypes in a carrier-specific manner in a dish. As such, this platform represents a promising VUS risk-assessment tool that can be used for assessing HCM-associated VUS specifically, and VUS in general, and thus significantly contribute to the arsenal of precision medicine tools available in this emerging field.

Keywords

VUS; HCM; CRISPR/Cas9; iPSCs

INTRODUCTION

Continued advancement in the field of medical genetics towards low-cost, and rapid next-generation sequencing has enabled increased genetic screening for disease-causing genetic mutations, not only in patients but also in “healthy” individuals. Because of this, genetic testing has uncovered a multitude of novel unclassified genetic variants, also known as variant(s) of unknown significance (VUS).[1, 2] A VUS is a genetic change for which pathogenicity has not been confirmed.[3] Consequently, clinical genetic testing often reports VUS with ambiguous and uncertain pathogenicity. This can cause anxiety and stress in otherwise asymptomatic individuals and families who are found to carry a VUS, especially when a poorly characterized variant is erroneously reported as “likely pathogenic” or even “pathogenic”.[4] VUS therefore poses serious clinical interpretation and risk-assessment challenges that limit the ability of healthcare providers to effectively counsel and treat individuals with unclear genetic predisposition to disease.

Hypertrophic cardiomyopathy (HCM), a common cause of sudden cardiac death (SCD), is a heterogeneous disease with vast genetic variability in the human genome, including a high degree of novel (“private”) mutations.[5] The findings of numerous VUS associated with HCM in “healthy” populations have created ambiguity in genetic test reports, posing a growing and unresolved challenge for cardiovascular precision medicine.[6] *In silico* tools such as PolyPhen2,[7] AlignGVGD,[8] and SIFT[9] have been developed to enable the prediction of the pathogenic likelihood of gene mutations by attempting to calculate the possible impact of an amino acid substitution on protein damage. However, these are only *in silico* predictions, and a variant classified as “likely pathogenic” or even “pathogenic” may actually be benign.[10] Hence, it is imperative to develop new experimental systems, ideally of

human origin, which can help assess the functional pathogenic potential of a VUS in a patient-specific manner.

In the case of heart disease, recent advances in induced pluripotent stem cell (iPSC) biology are generating groundbreaking opportunities for the study of genetic cardiomyopathy and familial arrhythmogenic syndromes such as Long QT,[11] catecholaminergic polymorphic ventricular tachycardia (CPVT),[12] Brugada syndrome[13] and HCM.[14, 15] Cardiomyocytes derived from iPSCs (iPSC-CMs) enable recapitulation of abnormal pathogenic cardiac phenotypes in a disease- and patient-specific manner.[16] Further strengthening this "disease in a dish" platform, the field of genome editing now allows interrogation of genetic mutations via genotype-phenotype correlation in a patient-specific manner using iPSCs.[17–20] With the aid of clustered regularly interspaced short palindromic repeats/Cas9 (CRISPR/Cas9) and single-stranded oligodeoxynucleotide (ssODN) mediated genome editing technologies, a genetic mutation can be readily introduced or corrected in iPSCs to create isogenic patient-specific iPSC lines in a dish.[21, 22] The generated isogenic iPSC lines share the same genetic background and differ exclusively at the mutation site. This advantage eliminates confounding factors due to different genetic backgrounds, allowing the genotype-phenotype relationship to be deciphered in a more precise and measurable manner. Taken together, the powerful combination of iPSC-based disease modeling and tools such as CRISPR/Cas9-mediated genome editing present an unprecedented opportunity to study VUS functional phenotypes in a patient-specific manner.

To highlight the potential application of CRISPR/Cas9 and iPSC disease models to clinical genetic testing, we have chosen to study a VUS with contradictory genotype-phenotype reports. The VUS is a missense variant (NM_000258.2:c.170C>A, NP_000249.1:p.Ala57Asp) in *MYL3*, a protein-coding gene that is a prominent component of the sarcomere complex.[23] The VUS was discovered in an asymptomatic carrier without clinical nor family history (3 generations) associated with suspicion of cardiac disease and sudden cardiac death (SCD). Despite the asymptomatic nature of the individual, this VUS is surprisingly predicted with confidence using *in silico* tools to be pathogenically damaging to protein function. Moreover, conflicting interpretations of pathogenicity are reported in the ClinVar database.[24] Some genetic testing resources classify this variant as a VUS, while others classify it as a likely pathogenic mutation having the potential to cause HCM. In this study, we use a combined CRISPR/Cas9-iPSC approach to evaluate the pathogenicity of this HCM-associated VUS. These approaches will be critical in the future to mitigate patient and family anxiety when they are confronted with unclear genetic predisposition to a disease, allowing more targeted therapies to reduce unnecessary harmful medical interventions and testing while cutting cost.

METHODS

Detailed methods are available in the Data Supplement. The data, analytic methods, and study materials for the purposes of reproducing the results or replicating procedures can be made upon request to the corresponding author who manages the information.

Genomic variant detection in heart disease-related genes

The study was carried out under Stanford Institutional Review Board (IRB) and that the subjects gave informed consent. 54 healthy subjects without cardiac-disease clinical history and presenting with normal ECG and echocardiography findings were recruited by the Stanford Cardiovascular Institute Biobank. Genetic testing of these subjects for this study was approved by Stanford University Institutional Review Board. Genomic DNA was isolated using DNeasy Blood and Tissue kits (Qiagen). Ion Torrent libraries from the 54 individual DNA samples were prepared with the Ion AmpliSeq™ Kit for Chef DL8 (Thermo Fisher Scientific) using a custom AmpliSeq panel (Thermo Fisher Scientific), which covers 135 cardiomyopathy and congenital heart disease DNA panel genes associated with sudden cardiac death.[25] Next, the libraries were sequenced on an Ion PI™ Chip (Thermo Fisher Scientific) with the Ion Proton system using the Ion PI™ Hi-Q™ Sequencing 200 Kit (Thermo Fisher Scientific). Sequence reads were aligned to human genome hg19 using Ion Torrent Suite Software (v5.0) and genomic variants were detected by Torrent Variant Caller plugin. VCF files of all samples were then annotated by Ion Reporter (ionreporter.thermofisher.com). Annotations of genetic variants were from ClinVar.[24]

iPSC Generation

The study was carried out under Stanford Institutional Review Board (IRB) and Stem Cell Research Oversight (SCRO) Committee guidelines and that the subjects gave informed consent. Patients' peripheral blood mononuclear cells (PBMCs) were collected and reprogrammed from a $MYL3_{(170C>A)}$ VUS carrier, a $MYBPB3_{(961G>A)}$ variant carrier, and two healthy individuals[26] using the CytoTune™-iPS 2.0 Sendai Reprogramming Kit (Thermo Fisher Scientific).

Genome Editing

iPSCs were transfected with CRISPR/Cas9 and ssODN using the Lipofectamine 3000 Reagent (Thermo Fisher Scientific). For each well of a 6-well plate, 1 μg CRISPR/Cas9 vectors and 4 μg ssODN were used for transfection. For each genome edited line (isogenic corrected, isogenic homozygous VUS $MYL3_{(170C>A)}$, frameshift mutation $MYL3^{(170C>A/fs)}$, and isogenic heterozygous $MYL3_{(170C>G)}$), several clones were generated, three of which were continuously propagated and used for cardiomyocytes differentiation and characterization.

Statistical Analysis

For statistical analysis, Student's t-test was used to compare the difference between two data sets. For comparison among multiple groups, one-way or two-way ANOVA was used, where appropriate, and Holm-Sidak or Tukey after-tests were used for all pairwise comparisons, depending on the properties of the data sets. A P value <0.05 was considered to be statistically significant. The presented data was derived from three replicates, acquired from three differentiations performed on three separate occasions. All data in bar graphs were presented as mean ± standard error mean.

RESULTS

Uncovering a likely pathogenic HCM variant in an asymptomatic individual

We recruited 54 healthy individuals without clinical suspicion for heart disease from the Stanford Cardiovascular Institute iPSC Biobank, then sequenced their DNA using a custom 135 cardiomyopathy and congenital heart disease DNA panel genes associated with sudden cardiac death to determine whether they carried “pathogenic” or “likely pathogenic” mutations.[25] Based on the ClinVar annotations[24] of the resulting 592 unique non-synonymous genetic variants across these 54 individuals, the majority (78%) were categorized as benign, likely benign or VUS (Supplemental Figure S1A). Interestingly, 17 individuals each carried one variant annotated as “likely pathogenic”, among them 4 individuals carried a “likely pathogenic” HCM-related VUS (Supplemental Table S1).

Further complicating these conflicting variant findings is the fact that most individuals lack detailed family clinical histories. Out of the 4 identified “likely pathogenic” HCM VUS individuals, only one individual had multigenerational family members that were available and willing to undergo further echocardiography, authorize open access to their clinical and family history, and agree to a direct interview, in addition to genetic screening. We therefore chose to study this individual’s missense variant, (NM_000258.2:c.170C>A, NP_000249.1:p.Ala57Asp) in the sarcomeric gene *MYL3* (Figure 1A, 1B). Importantly, this variant has not been previously reported in the literature and presents conflicting ClinVar reports, with some classifying the variant as a VUS and others as likely pathogenic (Table 1).[24]

MYL3 gene encodes MYL3 protein, which is an important modulator of sarcomeric myosin cross-bridge kinetics essential for the modulation of cardiac muscle contraction.[23] The A57D variant is a non-conservative amino acid substitution (Figure 1C), which is likely to affect secondary protein structure as these residues differ in polarity, charge, size, and other properties.[27] Missense variants in nearby residue (E56G) and at the same residue (A57G) have been reported in the Human Gene Mutation Database in association with HCM (Figure 1A), further supporting the functional importance of this region of the protein and a strong association of this particular locus with the HCM disease.[28] The VUS$MYL3_{(170C>A)}$ was then evaluated using an *in silico* analysis tool, PolyPhen2, on a damaging score scale of 0-1, 0 being benign and 1 being pathogenic (damaging to the protein function).[7] Surprisingly, despite the asymptomatic cardiac history of the 46 years old VUS$MYL3_{(170C>A)}$ carrier, the *in silico* analysis tool displayed a high score of 0.998 (Figure 1D), confidently predicting the VUS$MYL3_{(170C>A)}$ to be pathogenic and very damaging to the function of the MYL3 protein. This was further validated using additional *in silico* tools (SIFT and AlignGVGD). Moreover, interrogation of this VUS$MYL3_{(170C>A)}$ using the Exome Aggregation Consortium (ExAC) database showed that this mutation is observed in only 14 out of 121,338 individuals (Supplemental Table S2), indicating again this variant is infrequent and likely pathogenic.

At the carrier level, an electrocardiogram (ECG) assessment was conducted and did not detect an abnormal phenotype (Figure 1E). Similarly, echocardiogram did not show any evidence of hypertrophic cardiomyopathy (Table 2). To further assess the asymptomatic

nature of this HCM-associated VUS*MYL3*$_{(170C>A)}$, seven family members representing three generations underwent Sanger sequencing. Four of the seven family members, including the studied proband, (70, 48, 46, 11 years of age) were found to carry the "likely pathogenic" VUS*MYL3*$_{(170C>A)}$ in their genomes (Supplemental Figure S1B, 1C). Similar to the proband, none of them displayed any phenotypic evidence of HCM, as is depicted by their echocardiograph results in Table 2, nor proarrhythmic clinical history (e.g., syncope or resuscitation).

Generation of an isogenic corrected "healthy" control iPSC line using CRISPR/Cas9

One crucial limitation of patient-specific iPSCs as a unique tool for the study of human disease has been the inability to perform experiments under genetically defined conditions. This is particularly relevant for the study of this specific VUS*MYL3*$_{(170C>A)}$ case, as heterogeneous genetic background among individuals may disguise the subtle phenotype *in vitro* due to the asymptomatic nature of the VUS*MYL3*$_{(170C>A)}$ carrier. Accordingly, in addition to the control iPSC lines derived from two non-consanguineous healthy individuals,[26] an isogenic genetically corrected control line was generated from iPSCs of the heterozygous VUS*MYL3*$_{(170C>A)}$ carrier to help evaluate disease-relevant changes. The VUS*MYL3*$_{(170C>A)}$ carrier's peripheral blood mononuclear cells (PBMCs) were collected and reprogrammed to iPSCs (Supplemental Figure S2). CRISPR/Cas9 were then used to generate the isogenic corrected control cell line (Figures 2A, 2B). Three independent isogenic corrected clones were generated and confirmed by Sanger sequencing (Figure 2C, Supplemental Figure S3A). To exclude potential off-target cuttings by CRISPR/Cas9, ten genomic loci with the highest sequence homology to the guide RNA's binding site were checked by Sanger sequencing, separately for each one of the three clones. Sequencing results showed that the generated isogenic control cell line did not harbor any insertions or deletions at these loci (Supplemental Table S3).

Interrogation of cell morphology and gene expression of the heterozygous VUS*MYL3*$_{(170C>A)}$ iPSC-CMs

Multiple studies have reported myocyte sarcomere disarray and increased cell size to be features of HCM.[14, 15] Therefore, to test whether the heterozygous VUS*MYL3*$_{(170C>A)}$-iPSC-CMs display similar sarcomeric disarray and increased cell size, we conducted immunostaining of sarcomeric proteins and cell size measurements on the VUS*MYL3*$_{(170C>A)}$-iPSC-CMs and compared it to the two healthy controls and isogenic corrected control (consisting of 3 clones) iPSC-CMs (Supplemental Figure S3B, 3C). Interestingly, immunostaining using sarcomere protein antibody anti-cardiac troponin T and anti sarcomeric-α-Actinin showed that the heterozygous VUS*MYL3*$_{(170C>A)}$-iPSC-CMs display normal sarcomere distribution, similar to the two healthy controls and isogenic control iPSC-CM counterparts (Figure 3A, Supplemental Figure S3D). Furthermore, cell size analysis revealed no significant differences in cell size distribution and average cell area among the tested iPSC-CM lines (healthy controls, isogenic corrected control, and heterozygous VUS*MYL3*$_{(170C>A)}$) (Figure 3B, 3C, 3D, Supplemental Figure S3E). Overall, iPSC-CMs carrying the HCM-associated VUS*MYL3*$_{(170C>A)}$ do not express HCM-relevant abnormal morphological features.

Cardiomyocytes derived from HCM patients upregulate natriuretic peptide precursor A (NPPA) expression and have high β-myosin/α-myosin ratios.[14, 29] In addition, HCM patient-specific iPSC-CMs were previously reported to display upregulated expression of a group of genes that include *NPPA*, *TNNT2*, *MYL2*, *MYL4*, and *MYH7*.[14, 15] Accordingly, gene expression analysis was performed on the VUS*MYL3*$_{(170C>A)}$-iPSC-CMs at 45-50 days post-differentiation (dpd). The heterozygous VUS*MYL3*$_{(170C>A)}$-iPSC-CMs displayed normal gene expression similar to their control counterparts, exhibiting no increased expression of the aforementioned genes, nor an elevation of the β-myosin/α-myosin ratio (Figure 3E, Supplemental Figure S4). Next, we further interrogated the potential effect of the VUS*MYL3*$_{(170C>A)}$ on the expression level of additional myosin light chain (*MYL*) genes that are highly expressed in cardiomyocytes (*MYL3*, *MYL6*, *MYL7* and *MYL9*).[30] Interestingly, the heterozygous VUS*MYL3*$_{(170C>A)}$-iPSC-CMs expressed normal gene expression for all the tested myosin light chain genes (Figure 3E, Supplemental Figure S4). Altogether, these data show that the VUS*MYL3*$_{(170C>A)}$-iPSC-CMs do not display the HCM-associated phenotype at the gene expression level.

Functional assessments of the heterozygous VUS*MYL3*$_{(170C>A)}$ iPSC-CMs

HCM is caused by mutations in sarcomere genes. As such, HCM-related changes in the molecular sarcomeric motor apparatus impair cardiac function, in many cases leading to increased contractility.[31, 32] To test for potential MYL3 mutation-related functional alterations in the contractile apparatus of VUS*MYL3*$_{(170C>A)}$-iPSC-CMs, contractility assays were performed. Similar to the healthy control and isogenic corrected control lines, the heterozygous VUS*MYL3*$_{(170C>A)}$-iPSC-CMs displayed comparable contractility phenotype (Figure 4A), without any abnormal changes in beating rate, contraction and relaxation velocities (Figure 4B, 4C, 4D, Supplemental Figure S5A), contraction-relaxation distance, or contraction-relaxation duration (Supplemental Figure S5B).

Arrhythmia is a clinical hallmark of HCM.[33, 34] Recent studies demonstrated the ability of patient- and disease-specific iPSC-CMs to recapitulate this abnormal electrophysiological phenotype using the iPSC technology.[14, 15] Accordingly, VUS*MYL3*$_{(170C>A)}$-iPSC-CMs were electrophysiologically assessed using a fluorescent voltage sensor with fast kinetics for imaging high-frequency electrical activity, applied as a membrane voltage change indicator, known as accelerated sensor of action potentials (ASAP).[35] The VUS*MYL3*$_{(170C>A)}$-iPSC-CMs did not display a clear proarrhythmic potential (Figure 4E), with only 8% of the heterozygous VUS*MYL3*$_{(170C>A)}$-iPSC-CMs displaying delayed afterdepolarizations (DADs), a percentage similar to that detected in two healthy controls and isogenic corrected control lines (4%, 10%, and 9%, respectively) (Figure 4F, Supplemental Figure S5C). In summary, in contrast to the *in silico* pathogenic prediction, the lack of proarrhythmic activity presented by the VUS*MYL3*$_{(170C>A)}$-iPSC-CMs clearly reflects the asymptomatic nature of the VUS*MYL*$_{(170C>A)}$ carrier.

Previous studies interrogating the various mechanisms underlying arrhythmia in patients with HCM have implicated abnormal Ca^{2+} homeostasis as one of the proarrhythmic mediators.[36, 37] A recent study conducted on patient-specific HCM iPSC-CMs also revealed high levels of diastolic Ca^{2+}, contributing to the disease proarrhythmic nature.[14] To test for a

proarrhythmic Ca^{2+}-handling phenotype, we next recorded Ca^{2+} transients. Compared to the two healthy controls and the isogenic corrected control iPSC-CMs lines, the heterozygous VUS*MYL3*$_{(170C>A)}$-iPSC-CMs did not exhibit abnormal proarrhythmic Ca^{2+} transients (Figure 4G, 4H, Supplemental Figure S5D), in accordance with the previous electrophysiological findings. In conclusion, the genetic, morphological, and functional assessments of the heterozygous VUS*MYL3*$_{(170C>A)}$-iPSC-CMs all display an asymptomatic phenotype, similarly to that exhibited clinically by the VUS*MYL3*$_{(170C>A)}$ carrier.

Comprehensive analysis of a generated isogenic homozygous VUS*MYL3*$_{(170C>A)}$ iPSC line

The heterozygous VUS*MYL3*$_{(170C>A)}$-iPSC-CMs did not show a pathogenic phenotype, despite a high *in silico* assessment score confidently predicting it to be pathogenically damaging. This predicament may be the result of the VUS*MYL3*$_{(170C>A)}$ being a disease-causing variant in the recessive state, and therefore explains the lack of pathogenic phenotype observed at the iPSC-CMs level. Unfortunately, since this variant is a VUS by definition, there is no support for recessive inheritance of this VUS*MYL3*$_{(170C>A)}$. To overcome this possible predicament, we next created a homozygous VUS*MYL3*$_{(170C>A)}$ line using a CRISPR/Cas9 (Supplemental Figure S6A), generating three independent clones for characterization. Sanger sequencing confirmed that the heterozygous VUS*MYL3*$_{(170C>A)}$ line was turned into a homozygous VUS*MYL3*$_{(170C>A)}$ line (Figure 5A, Supplemental Figure S6B), and no off-target mutation was detected in the three homozygous VUS*MYL3*$_{(170C>A)}$ iPSC clones (Supplemental Table S4). Interestingly, genome-edited homozygous VUS*MYL3*$_{(170C>A)}$-iPSC-CMs displayed similar genetic, morphological, and functional assessment results, compared to those displayed by the heterozygous VUS*MYL3*$_{(170C>A)}$ and isogenic corrected control lines. The genome-edited homozygous VUS*MYL3*$_{(170C>A)}$-iPSC-CMs also did not exhibit the following: (1) elevation in HCM-related genes (Figure 5C, Supplemental Figure S7A); (2) alterations in the gene expression level of the aforementioned myosin light chain genes (Figure 5C, Supplemental Figure S7A) (3) increased cell size (Figure 5D, Supplemental Figure S7B); (4) disarray of sarcomere organization (Figure 5E, Supplemental Figure S7C); (5) alterations in contractility (Figure 5F-H, Supplemental Figure S7D-F); (6) electrophysiological proarrhythmic phenotype (Figure 5I, 5J, Supplemental Figure S7G); or (7) irregular Ca^{2+}-handling (Figure 5K, 5L, Supplemental Figure S7H). In conclusion, the lack of a pathogenic phenotype in all three individually generated genome-edited homozygous VUS*MYL3*$_{(170C>A)}$-iPSC-CMs clones, further supports the interpretation that the VUS*MYL3*$_{(170C>A)}$ variant is benign.

To further confirm the benign phenotype interpretation, we generated a premature stop codon (frameshift mutation) in the healthy *MYL3* allele of the heterozygous VUS*MYL3*$_{(170C>A)}$ cell line, thus generating a cell line that lacks a healthy *MYL3* allele (loss of heterozygosity) and thus only expresses the variant allele. Three individual frameshift mutation clones were generated using the same gRNA as the generation of the homozygous VUS*MYL3*$_{(170C>A)}$ line. To test the integrity of the frameshift mutation line, the presence of a premature stop codon in the *MYL3* gene was validated by Sanger sequencing of the genomic DNA (Figure 5B, Supplementary Figure S6C). Sanger sequencing of the RT-PCR product validated the degradation of the frameshift allele mRNA.

Thus only the mutated allele mRNA was identified (Supplementary Figure S6D). Next, three frameshift mutation clones were assessed at the genetic, morphological and functional levels, and compared to the heterozygous VUS*MYL3*$_{(170C>A)}$ and isogenic corrected control phenotypes. Similar to the homozygous VUS*MYL3*$_{(170C>A)}$ line, we found no evidence of a HCM phenotype in the frameshift mutation cell line (Figure 5C-L, Supplementary Figure S7A-H), further strengthening our conclusion that VUS*MYL3*$_{(170C>A)}$ is a benign genomic variant.

Comprehensive analysis of symptomatic HCM iPSC-CMs lines

To rule out the possibility that the benign prediction for the VUS*MYL3*$_{(170C>A)}$ was simply due to a lack of sensitivity on part of the iPSC-CMs platform, we next assayed two different HCM disease-associated mutations, displaying severe clinical HCM-related symptoms at the carrier level, in iPSC-CMs as positive controls. To validate that the benign assessment is not the result of the inability of the iPSC-CM platform to recapitulate a pathogenic *MYL3* mutation phenotype *in vitro*, a known autosomal dominant pathogenic mutation, *MYL3* c.170C>G, at the same nucleotide position as the VUS*MYL3*$_{(170C>A)}$, was studied. This mutation was reported to develop a severe HCM phenotype, including SCD, with disease penetrance in 78% of the genotyped *MYL3* c.170C>G mutation carriers, and an onset as early as 28 years of age.[27] For this purpose, the *MYL3* c.170C>G mutation was introduced into the heterozygous VUS*MYL3*$_{(170C>A)}$ iPSCs using CRISPR/Cas9 (Supplementary Figure S8A). Accordingly, three independent iPSC clones (named *MYL3*$_{(170C>G)}$) were generated and were tested by Sanger sequencing to confirm that the *MYL3* c.170C>A variant allele was replaced with the *MYL3* c.170C>G mutation (Figure 6A, Supplemental Figure S8B) without off-target cutting (Supplemental Table S5). Next, to further elucidate the capability of the iPSC-CMs platform to recapitulate a pathogenic phenotype of a symptomatic carrier, a heterozygous HCM missense genetic variant in the sarcomeric gene *MYBPC3* (*MYBPC3* c.961G>A, p.Val321Met) (Figure 6A) was studied using a carrier-specific iPSC-CMs line. Note that the carrier presented an early HCM onset at the young age of 23 (Table 2), is implanted with a cardioverter defibrillator, and has a strong family history of SCD, as early as 34 years of age.

The iPSC lines were then evaluated for pathogenic morphological changes and functional proarrhythmic potential. Similar to the heterozygous VUS*MYL3*$_{(170C>A)}$-iPSC-CMs, both *MYL3*$_{(170C>G)}$- and *MYBPC3*$_{(961G>A)}$-iPSC-CMs exhibited no significant difference in cell size (Figure 6B, Supplementary Figure S8C) and had normal sarcomere distribution (Supplementary Figure S8D). However, while heterozygous VUS*MYL3*$_{(170C>A)}$-iPSC-CMs displayed normal expression of HCM-related genes (*NPPA*, *TNNT2*, *MYL2*, and *MYH7*), these HCM-related genes, including the β-myosin/α-myosin ratio, were elevated in the *MYL3*$_{(170C>G)}$- and *MYBPC3*$_{(961G>A)}$-iPSC-CMs (Figure 6C, Supplementary Figure S8E). While both *MYL3*$_{(170C>G)}$- and *MYBPC3*$_{(961G>A)}$-iPSC-CMs did not exhibit a change in expression level of the myosin light chain genes (*MYL2, MYL3*, *MYL6*, *MYL7* and *MYL9*) in comparison to the isogenic corrected and heterozygous VUS*MYL3*$_{(170C>A)}$-iPSC-CMs, a significant increase in the MYL4 expression was noted (Figure 6C), as has been previously reported by multiple HCM-related studies.[38–40] Contractility measurements did not display a statistically significant difference in beating rate among the tested lines (Figure 6D,

Supplementary Figure S8F). Both *MYL3*$_{(170C>G)}$- and *MYBPC3*$_{(961G>A)}$-iPSC-CMs displayed faster contraction velocity in comparison to the corrected isogenic control line and heterozygous VUS*MYL3*$_{(170C>A)}$-iPSC-CMs (Figure 6E, Supplementary Figure S8F). *MYL3*$_{(170C>G)}$-iPSC-CMs displayed faster relaxation velocity (Figure 6F, Supplemental Figure S8F), as previously documented for this specific *MYL3*$_{(170C>G)}$ gene mutation,[41, 42] and as validated in this study by three independent *MYL3*$_{(170C>G)}$-iPSC-CMs clones. The *MYBPC3*$_{(961G>A)}$-iPSC-CMs did not exhibit a significant difference in relaxation velocity compared with the isogenic corrected control and heterozygous VUS*MYL3*$_{(170C>A)}$-iPSC-CMs (Figure 6F). Notably, while only 8% of heterozygous VUS*MYL3*$_{(170C>A)}$-iPSC-CMs displayed a proarrhythmic electrophysiological phenotype in the form of DADs (Figure 4F), 42% and 46% of the *MYL3*$_{(170C>G)}$- and *MYBPC3*$_{(961G>A)}$-iPSC-CMs, respectively, exhibited DADs, displaying higher amplitude and shorter coupling intervals (Figure 6G, 6I, Supplemental Figure S8G). In addition, both presented significant variability in beat-to-beat intervals of action potentials (Figure 6H), another notable proarrhythmic characteristic. In accordance with the electrophysiological findings, 37% and 47% of the *MYL3*$_{(170C>G)}$- and *MYBPC3*$_{(961G>A)}$-iPSC-CMs, respectively, exhibited an abnormal Ca^{2+} phenotype, presenting double-peaked Ca^{2+} transients (Figure 6J, K, Supplemental Figure S8H) that was previously shown to be a proarrhythmic manifestation in HCM iPSC-CM[14] as well as in another familial arrhythmogenic syndrome iPSC-CM study.[12] These events were virtually absent in the VUS*MYL3*$_{(170C>A)}$-iPSC-CMs. Importantly, Fura2 Ca^{2+} imaging further demonstrated a significant increase in diastolic Ca^{2+} in both *MYL3*$_{(170C>G)}$- and *MYBPC3*$_{(961G>A)}$-iPSC-CMs, when compared to the corrected and heterozygous VUS*MYL3*$_{(170C>A)}$-iPSC-CMs lines (Supplementary Figure S8I).

Taken together, similarly to the symptomatic nature of both *MYL3*$_{(170C>G)}$ and *MYBPC3*$_{(961G>A)}$ carriers, an evident symptomatic functional phenotype was recapitulated by the *MYL3*$_{(170C>G)}$- and *MYBPC3*$_{(961G>A)}$-iPSC-CMs, respectively, highlighting the potential of the iPSC-CM platform to successfully assess both pathogenic and benign phenotypes.

DISCUSSION

In this study, we combine the powerful strengths of iPSC-based disease modeling and CRISPR/Cas9-mediated genome editing technology to demonstrate their unique potential as a personalized VUS risk-assessment platform for determining the pathogenicity of VUS. To highlight the dilemma and uncertainty that VUS presents for patients and clinicians around the world, we screened dozens of “healthy” individuals in search of a VUS that can clearly showcase the uncertainty surrounding genomic variant interpretation: a variant in a healthy individual that is annotated as “likely pathogenic”. By combining both aforementioned technologies for the study of such a VUS (*MYL3* c.170C>G associated with HCM), we were able to: 1) recapitulate the asymptomatic phenotype of the VUS*MYL3*$_{(170C>A)}$ carrier by showing a lack of HCM-related gene expression profile, morphological phenotype, and proarrhythmic activity in the heterozygous VUS*MYL3*$_{(C>A)}$-iPSC-CMs; 2) confirm the asymptomatic clinical phenotype as a benign assessment in a genome-edited isogenic homozygous VUS*MYL3*$_{(170C>A)}$ line, as well as in a heterozygous frameshift mutation

MYL3$^{(170C>A/fs)}$ line; 3) validate the ability of the combined iPSC-CMs and genome-editing platform to recapitulate a pathogenic phenotype of a symptomatic carrier.

HCM is a prevalent hereditary cardiac disorder linked by both animal models and patient-specific iPSC-CMs studies to arrhythmia and SCD.[14, 15, 43] In contrast to these models, the carrier-specific VUS*MYL3*$_{(170C>A)}$-iPSC-CMs did not display a proarrhythmic phenotype. To validate whether the observed asymptomatic nature of the VUS*MYL3*$_{(170C>A)}$-iPSC-CMs is the result of a recessive missense mutation, we also generated a homozygous VUS*MYL3*$_{(170C>A)}$ line. Interestingly, similar to the heterozygous cells, the phenotype displayed by all three homozygous iPSC-CMs clones was an asymptomatic one as well. The asymptomatic assessment of the homozygous line was further strengthened by an asymptomatic phenotype detected in the genome-edited heterozygous frameshift mutation *MYL3*$^{(170C>A/fs)}$ line (expressing solely the c.170C>A variant allele). Collectively, these data confirm that the lack of pathogenic phenotype in heterozygous VUS*MYL3*$_{(170C>A)}$-iPSC-CMs was not the result of a recessive gene.

HCM is a complex and heterogeneous disease encompassing a wide variety of mutations and variants.[29, 32] To validate whether the benign asymptomatic assessments of both the heterozygous VUS*MYL3*$_{(170C>A)}$ and the genome-edited homozygous VUS*MYL3*$_{(170C>A)}$-iPSC-CMs are not the result of a potential inability on part of the iPSC-CMs platform to recapitulate a pathogenic *MYL3* mutation phenotype, we next genome-edited iPSCs with a known disease-causing mutation in the *MYL3* gene (*MYL3* c.170C>G), at the same nucleotide position as the VUS*MYL3*$_{(170C>A)}$[27]. Next, to further test the sensitivity of this cellular platform to recapitulate a HCM VUS, iPSCs from an HCM patient with a *MYBPC3* c.961G>A variant were generated from a carrier presenting classical clinical HCM symptoms. We found that both the *MYL3*$_{(170C>G)}$- and *MYBPC3*$_{(961G>A)}$-iPSC-CMs did show a HCM pathogenic phenotype, for example upregulation of HCM-related genes expression, elevation in β-myosin/α-myosin ratio, irregular contractility, proarrhythmic electrophysiological phenotype (DADs), and an abnormal Ca^{2+} phenotype, similar to the results from previous HCM iPSC-CMs and HCM animal studies.[14, 15, 41, 44, 45] The HCM-related phenotypes observed in both the *MYL3*$_{(170C>G)}$- and *MYBPC3*$_{(961G>A)}$-iPSC-CMs, effectively demonstrate that the lack of phenotype exhibited by both the heterozygous and homozygous VUS*MYL3*$_{(170C>A)}$-iPSC-CMs was not due to a technical artifact or faulty detection sensitivity on part of the iPSC-CMs platform, but rather a reflection of a benign phenotype.

Over the past decade, a large range of studies, using similar assays to those presented in the current study, have demonstrated the intriguing ability of the iPSC-CMs platform to recapitulate disease phenotype presented by the patient at bedside at the patient-derived cellular level in the dish, as been previously reported for genetic cardiomyopathy and arrhythmogenic syndromes such as: LQT, CPVT, Brugada syndrome, familial dilated cardiomyopathy (DCM), and HCM.[11, 12, 14, 15, 46] Similarly, iPSC-CMs have been also shown to recapitulate a normal “healthy” phenotype in cells derived from “healthy” subjects, as documented by countless studies. This striking recapitulation capability of the iPSC-CMs platform is also vivid in this study. The chosen carrier is a healthy 46 years old active, athletic, healthy individual, that although has been phenotyped with a “likely pathogenic”

HCM *MYL3* c.170C>A VUS, does not have a clinical cardiac history, presents normal ECG, and normal echocardiography results. Further, supporting the asymptomatic nature of the carrier is the carrier's impressive family history, consisting of 3 generations of asymptomatic carriers as old as 70 years of age. Impressively, the proband derived-cells reflect the proband's asymptomatic nature. In a similar manner, in the case of the $MYL3_{(170C>G)}$ mutation, the cells also strikingly recapitulated the carriers' clinical phenotype. $MYL3_{(170C>G)}$ mutation carriers have been shown to experience HCM-related symptoms including SCD, with disease penetrance of 78% and an onset as early as 28 and as late as 38 years of age. The genome-edited $MYL3_{(170C>G)}$-iPSC-CMS nicely recapitulate the symptomatic nature of the carriers. Reinforcing these findings, an additional carrier displaying a HCM variant demonstrating a clinical HCM onset as early as 23 years of age and a family history of SCD at an age as young as 34, was studied. In this case, the carrier-derived iPSC-CMs were also able to recapitulate a pathogenic phenotype. Altogether, the presented evidence here demonstrates the capability of the carrier-specific iPSC-CMs platform to reveal both a benign and pathogenic phenotype of prospective variants in a manner that recapitulates the carrier's clinical presentation.

Collectively, our data demonstrate the unique potential of combining iPSC-based disease modeling and CRISPR/Cas9-mediated genome editing technology as a personalized VUS risk-assessment platform that can facilitate the study of the growing VUS phenomenon. Linking together iPSC and genome editing technologies presents an unprecedented opportunity to elucidate the pathogenicity of VUS in a dish in a carrier-specific manner. Importantly, these efforts will help improve the study and diagnostics of VUS specifically and the promotion of personalized and precision medicine in general, better guiding clinicians in their choice of therapy and providing a clearer result for the VUS carriers.

Supplementary Material

Refer to Web version on PubMed Central for supplementary material.

Acknowledgments

We would like to thank Blake Wu for editing the manuscript. We thank Andrew Olson from Stanford Neuroscience Microscopy Service (NMS), Jon Mulholland and Cedric Espenel from Stanford Cell Sciences Imaging Facility (CSIF) for their help with confocal imaging.

FUNDING SOURCES

This study was funded by Stanford Frankenstein@200 grant (HC), the National Institutes of Health (NIH) grants K08 HL119251 (KDW), R01 HL126527, R01 HL130020, and R01 HL113006 (JCW).

References

1. Richards S, Aziz N, Bale S, Bick D, Das S, Gastier-Foster J, Grody WW, Hegde M, Lyon E, Spector E, Voelkerding K, Rehm HL, Comm ALQA. Standards and guidelines for the interpretation of sequence variants: a joint consensus recommendation of the American College of Medical Genetics and Genomics and the Association for Molecular Pathology. Genet Med. 2015; 17:405–424. [PubMed: 25741868]
2. Eccles BK, Copson E, Maishman T, Abraham JE, Eccles DM. Understanding of BRCA VUS genetic results by breast cancer specialists. BMC Cancer. 2015; 15:936. [PubMed: 26608569]

3. Kobayashi Y, Yang S, Nykamp K, Garcia J, Lincoln SE, Topper SE. Pathogenic variant burden in the ExAC database: an empirical approach to evaluating population data for clinical variant interpretation. Genome Med. 2017; 9:13. [PubMed: 28166811]

4. Petrucelli N, Lazebnik N, Huelsman KM, Lazebnik RS. Clinical interpretation and recommendations for patients with a variant of uncertain significance in BRCA1 or BRCA2: A survey of genetic counseling practice. Genet Test. 2002; 6:107–113. [PubMed: 12215249]

5. Maron BJ, Maron MS, Semsarian C. Genetics of Hypertrophic cardiomyopathy after 20 years clinical perspectives. J Am Coll Cardiol. 2012; 60:705–715. [PubMed: 22796258]

6. Roma-Rodrigues C, Fernandes AR. Genetics of hypertrophic cardiomyopathy: advances and pitfalls in molecular diagnosis and therapy. The Application of Clinical Genetics. 2014; 7:195–208. [PubMed: 25328416]

7. Adzhubei IA, Schmidt S, Peshkin L, Ramensky VE, Gerasimova A, Bork P, Kondrashov AS, Sunyaev SR. A method and server for predicting damaging missense mutations. Nat Methods. 2010; 7:248–249. [PubMed: 20354512]

8. Juang JM, Lu TP, Lai LC, Hsueh CH, Liu YB, Tsai CT, Lin LY, Yu CC, Hwang JJ, Chiang FT, Yeh SS, Chen WP, Chuang EY, Lai LP, Lin JL. Utilizing multiple in silico analyses to identify putative causal SCN5A variants in Brugada syndrome. Sci Rep. 2014; 4:3850. [PubMed: 24463578]

9. Arora S, Huwe PJ, Sikder R, Shah M, Browne AJ, Lesh R, Nicolas E, Deshpande S, Hall MJ, Dunbrack RL Jr, Golemis EA. Functional analysis of rare variants in mismatch repair proteins augments results from computation-based predictive methods. Cancer Biol Ther. 2017; 18:519–533. [PubMed: 28494185]

10. Adzhubei I, Jordan DM, Sunyaev SR. Predicting functional effect of human missense mutations using PolyPhen-2. Curr Protoc Hum Genet. 2013

11. Itzhaki I, Maizels L, Huber I, Zwi-Dantsis L, Caspi O, Winterstern A, Feldman O, Gepstein A, Arbel G, Hammerman H, Boulos M, Gepstein L. Modelling the long QT syndrome with induced pluripotent stem cells. Nature. 2011; 471:225–229. [PubMed: 21240260]

12. Itzhaki I, Maizels L, Huber I, Gepstein A, Arbel G, Caspi O, Miller L, Belhassen B, Nof E, Glikson M, Gepstein L. Modeling of catecholaminergic polymorphic ventricular tachycardia with patient-specific human-induced pluripotent stem cells. J Am Coll Cardiol. 2012; 60:990–1000. [PubMed: 22749309]

13. Liang P, Sallam K, Wu H, Li Y, Itzhaki I, Garg P, Zhang Y, Vermglinchan V, Lan F, Gu M, Gong T, Zhuge Y, He C, Ebert AD, Sanchez-Freire V, Churko J, Hu S, Sharma A, Lam CK, Scheinman MM, Bers DM, Wu JC. Patient-specific and genome-edited induced pluripotent stem cell-derived cardiomyocytes elucidate single-cell phenotype of Brugada syndrome. J Am Coll Cardiol. 2016; 68:2086–2096. [PubMed: 27810048]

14. Lan F, Lee AS, Liang P, Sanchez-Freire V, Nguyen PK, Wang L, Han L, Yen M, Wang Y, Sun N, Abilez OJ, Hu S, Ebert AD, Navarrete EG, Simmons CS, Wheeler M, Pruitt B, Lewis R, Yamaguchi Y, Ashley EA, Bers DM, Robbins RC, Longaker MT, Wu JC. Abnormal calcium handling properties underlie familial hypertrophic cardiomyopathy pathology in patient-specific induced pluripotent stem cells. Cell Stem Cell. 2013; 12:101–113. [PubMed: 23290139]

15. Han L, Li Y, Tchao J, Kaplan AD, Lin B, Li Y, Mich-Basso J, Lis A, Hassan N, London B, Bett GC, Tobita K, Rasmusson RL, Yang L. Study familial hypertrophic cardiomyopathy using patient-specific induced pluripotent stem cells. Cardiovasc Res. 2014; 104:258–269. [PubMed: 25209314]

16. Wilson KD, Wu JC. Induced pluripotent stem cells. Jama-J Am Med Assoc. 2015; 313:1613–1614.

17. Hendriks WT, Warren CR, Cowan CA. Genome editing in human pluripotent stem cells: approaches, pitfalls, and solutions. Cell Stem Cell. 2016; 18:53–65. [PubMed: 26748756]

18. Hockemeyer D, Jaenisch R. Induced pluripotent stem cells meet genome editing. Cell Stem Cell. 2016; 18:573–586. [PubMed: 27152442]

19. Ma N, Liao BJ, Zhang H, Wang LL, Shan YL, Xue YT, Huang K, Chen SB, Zhou XX, Chen Y, Pei DQ, Pan GJ. Transcription activator-like effector nuclease (TALEN)-mediated gene correction in integration-free beta-thalassemia induced pluripotent stem cells. Journal of Biological Chemistry. 2013; 288:34671–34679. [PubMed: 24155235]

20. Ma N, Shan YL, Liao BJ, Kong GY, Wang C, Huang K, Zhang H, Cai XJ, Chen SB, Pei DQ, Chen NS, Pan GJ. Factor-induced reprogramming and zinc finger nuclease-aided gene targeting cause

different genome instability in β-thalassemia induced pluripotent stem cells (iPSCs). Journal of Biological Chemistry. 2015; 290:12079–12089. [PubMed: 25795783]

21. Richardson CD, Ray GJ, DeWitt MA, Curie GL, Corn JE. Enhancing homology-directed genome editing by catalytically active and inactive CRISPR-Cas9 using asymmetric donor DNA. Nat Biotechnol. 2016; 34:339–344. [PubMed: 26789497]
22. Paquet D, Kwart D, Chen A, Sproul A, Jacob S, Teo S, Olsen KM, Gregg A, Noggle S, Tessier-Lavigne M. Efficient introduction of specific homozygous and heterozygous mutations using CRISPR/Cas9. Nature. 2016; 533:125–129. [PubMed: 27120160]
23. Hernandez OM, Jones M, Guzman G, Szczesna-Cordary D. Myosin essential light chain in health and disease. Am J Physiol Heart Circ Physiol. 2007; 292:H1643–1654. [PubMed: 17142342]
24. Landrum MJ, Lee JM, Benson M, Brown GR, Chao C, Chitipiralla S, Gu B, Hart J, Hoffman D, Jang W, Karapetyan K, Katz K, Liu C, Maddipatla Z, Malheiro A, McDaniel K, Ovetsky M, Riley G, Zhou G, Holmes JB, Kattman BL, Maglott DR. ClinVar: improving access to variant interpretations and supporting evidence. Nucleic Acids Res. 2018; 46:D1062–D1067. [PubMed: 29165669]
25. Wilson KD, Shen P, Fung E, Karakikes I, Zhang A, InanlooRahatloo K, Odegaard J, Sallam K, Davis RW, Lui GK, Ashley EA, Scharfe C, Wu JC. A rapid, high-quality, cost-effective, comprehensive and expandable targeted next-generation sequencing assay for inherited heart diseases. Circ Res. 2015; 117:603–611. [PubMed: 26265630]
26. Sharma A, Burridge PW, McKeithan WL, Serrano R, Shukla P, Sayed N, Churko JM, Kitani T, Wu H, Holmstrom A, Matsa E, Zhang Y, Kumar A, Fan AC, Del Alamo JC, Wu SM, Moslehi JJ, Mercola M, Wu JC. High-throughput screening of tyrosine kinase inhibitor cardiotoxicity with human induced pluripotent stem cells. Sci Transl Med. 2017; 9:eaaaf2584.
27. Lee W, Hwang TH, Kimura A, Park SW, Satoh M, Nishi H, Harada H, Toyama J, Park JE. Different expressivity of a ventricular essential myosin light chain gene Ala57Gly mutation in familial hypertrophic cardiomyopathy. Am Heart J. 2001; 141:184–189. [PubMed: 11174330]
28. Andersen PS, Hedley PL, Page SP, Syrris P, Moolman-Smook JC, McKenna WJ, Elliott PM, Christiansen M. A novel myosin essential light chain mutation causes hypertrophic cardiomyopathy with late onset and low expressivity. Biochem Res Int. 2012; 2012:685108. [PubMed: 22957257]
29. Seidman JG, Seidman C. The genetic basis for cardiomyopathy: from mutation identification to mechanistic paradigms. Cell. 2001; 104:557–567. [PubMed: 11239412]
30. England J, Loughna S. Heavy and light roles: myosin in the morphogenesis of the heart. Cell Mol Life Sci. 2013; 70:1221–1239. [PubMed: 22955375]
31. Belus A, Piroddi N, Scellini B, Tesi C, Amati GD, Girolami F, Yacoub M, Cecchi F, Olivotto I, Poggesi C. The familial hypertrophic cardiomyopathy-associated myosin mutation R403Q accelerates tension generation and relaxation of human cardiac myofibrils. J Physiol-London. 2008; 586:3639–3644. [PubMed: 18565996]
32. Marsiglia JD, Pereira AC. Hypertrophic cardiomyopathy: how do mutations lead to disease? Arq Bras Cardiol. 2014; 102:295–304. [PubMed: 24714796]
33. Maron BJ. Hypertrophic cardiomyopathy: a systematic review. JAMA. 2002; 287:1308–1320. [PubMed: 11886323]
34. Maron BJ, Shirani J, Poliac LC, Mathenge R, Roberts WC, Mueller FO. Sudden death in young competitive athletes. Clinical, demographic, and pathological profiles. JAMA. 1996; 276:199–204. [PubMed: 8667563]
35. Chamberland S, Yang HH, Pan MM, Evans SW, Guan S, Chavarha M, Yang Y, Salesse C, Wu H, Wu JC, Clandinin TR, Toth K, Lin MZ, St-Pierre F. Fast two-photon imaging of subcellular voltage dynamics in neuronal tissue with genetically encoded indicators. Elife. 2017; 6:e25690. [PubMed: 28749338]
36. Adabag AS, Maron BJ, Appelbaum E, Harrigan CJ, Buros JL, Gibson CM, Lesser JR, Hanna CA, Udelson JE, Manning WJ, Maron MS. Occurrence and frequency of arrhythmias in hypertrophic cardiomyopathy in relation to delayed enhancement on cardiovascular magnetic resonance. J Am Coll Cardiol. 2008; 51:1369–1374. [PubMed: 18387438]

37. Wolf CM, Moskowitz IP, Arno S, Branco DM, Semsarian C, Bernstein SA, Peterson M, Maida M, Morley GE, Fishman G, Berul CI, Seidman CE, Seidman JG. Somatic events modify hypertrophic cardiomyopathy pathology and link hypertrophy to arrhythmia. Proc Natl Acad Sci U S A. 2005; 102:18123–18128. [PubMed: 16332958]

38. Schaub MC, Hefti MA, Zuellig RA, Morano I. Modulation of contractility in human cardiac hypertrophy by myosin essential light chain isoforms. Cardiovasc Res. 1998; 37:381–404. [PubMed: 9614495]

39. Morano M, Zacharzowski U, Maier M, Lange PE, Alexi-Meskishvili V, Haase H, Morano I. Regulation of human heart contractility by essential myosin light chain isoforms. J Clin Invest. 1996; 98:467–473. [PubMed: 8755658]

40. Petzhold D, Lossie J, Keller S, Werner S, Haase H, Morano I. Human essential myosin light chain isoforms revealed distinct myosin binding, sarcomeric sorting, and inotropic activity. Cardiovasc Res. 2011; 90:513–520. [PubMed: 21262909]

41. Kazmierczak K, Paulino EC, Huang W, Muthu P, Liang J, Yuan CC, Rojas AI, Hare JM, Szczesna-Cordary D. Discrete effects of A57G-myosin essential light chain mutation associated with familial hypertrophic cardiomyopathy. Am J Physiol Heart Circ Physiol. 2013; 305:H575–589. [PubMed: 23748425]

42. Kazmierczak K, Yuan CC, Liang J, Huang W, Rojas AI, Szczesna-Cordary D. Remodeling of the heart in hypertrophy in animal models with myosin essential light chain mutations. Front Physiol. 2014; 5:353. [PubMed: 25295008]

43. Geisterfer-Lowrance AA, Christe M, Conner DA, Ingwall JS, Schoen FJ, Seidman CE, Seidman JG. A mouse model of familial hypertrophic cardiomyopathy. Science. 1996; 272:731–4. [PubMed: 8614836]

44. Marsiglia JDC, Pereira AC. Hypertrophic Cardiomyopathy: how do mutations lead to disease? Arq Bras Cardiol. 2014; 102:295–303. [PubMed: 24714796]

45. Witjas-Paalberends ER, Ferrara C, Scellini B, Piroddi N, Montag J, Tesi C, Stienen GJ, Michels M, Ho CY, Kraft T, Poggesi C, van der Velden J. Faster cross-bridge detachment and increased tension cost in human hypertrophic cardiomyopathy with the R403Q MYH7 mutation. J Physiol. 2014; 592:3257–3272. [PubMed: 24928957]

46. Sun N, Yazawa M, Liu J, Han L, Sanchez-Freire V, Abilez OJ, Navarrete EG, Hu S, Wang L, Lee A, Pavlovic A, Lin S, Chen R, Hajjar RJ, Snyder MP, Dolmetsch RE, Butte MJ, Ashley EA, Longaker MT, Robbins RC, Wu JC. Patient-specific induced pluripotent stem cells as a model for familial dilated cardiomyopathy. Sci Transl Med. 2012; 4:130ra47.

CLINICAL PERSPECTIVE

What is new?

- Our study demonstrates for the first time the unique potential of combining iPSC-based disease modeling and CRISPR/Cas9-mediated genome editing technology as a personalized risk-assessment platform for determining the pathogenicity of a variant of uncertain significance (VUS) in a patient-specific manner.

What are the clinical implications?

- This personalized risk-assessment platform will help improve the study and diagnostics of VUS specifically and the promotion of personalized and precision medicine in general, better guiding clinicians in their choice of therapy and providing a clearer result for VUS carriers.

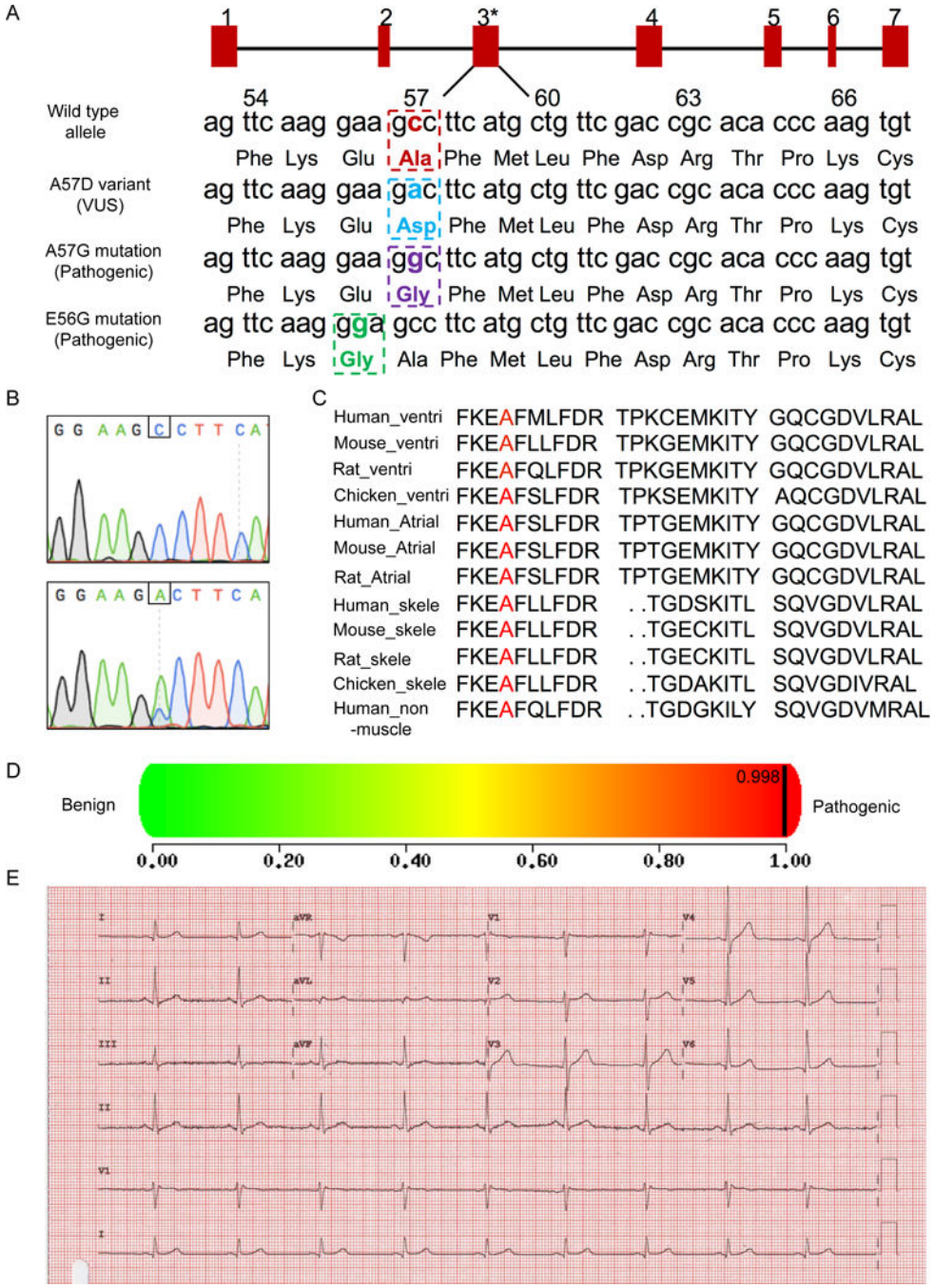

Figure 1. Confirmation of the likely pathogenic VUS*MYL3*$_{(170C>A)}$ uncovered in an asymptomatic carrier

(A) Schematic illustration of the nucleotide and amino acid position of the VUS (NM_000258.2:c.170C>A, NP_000249.1:p.Ala57Asp) and two known pathogenic mutations (A57G, E56G) in the *MYL*3 gene. The red rectangles represent exons 1-7. Asterisks displays VUS*MYL3*$_{(170C>A)}$ position. Numbers 54-66 annotate amino acids positions. (**B**) Sanger sequencing confirmation of the VUS*MYL3*$_{(170C>A)}$. Upper panel: Sequencing result of a healthy control individual, lower panel: sequencing result of the

heterozygous VUS*MYL3*$_{(170C>A)}$ carrier. Nucleotide position of the VUS*MYL3*$_{(170C>A)}$ is displayed by a framing square. (**C)** Alignment of regions flanking the VUS*MYL3*$_{(170C>A)}$ (red font) in MYL3 protein showing evolutionary conservation of the mutated residue across species and isoforms. (**D)** A prediction score of the VUS*MYL3*$_{(170C>A)}$ predicted by the *in silico* tool PolyPhen-2. **(E)** The VUS*MYL3*$_{(170C>A)}$ carrier's ECG recording.

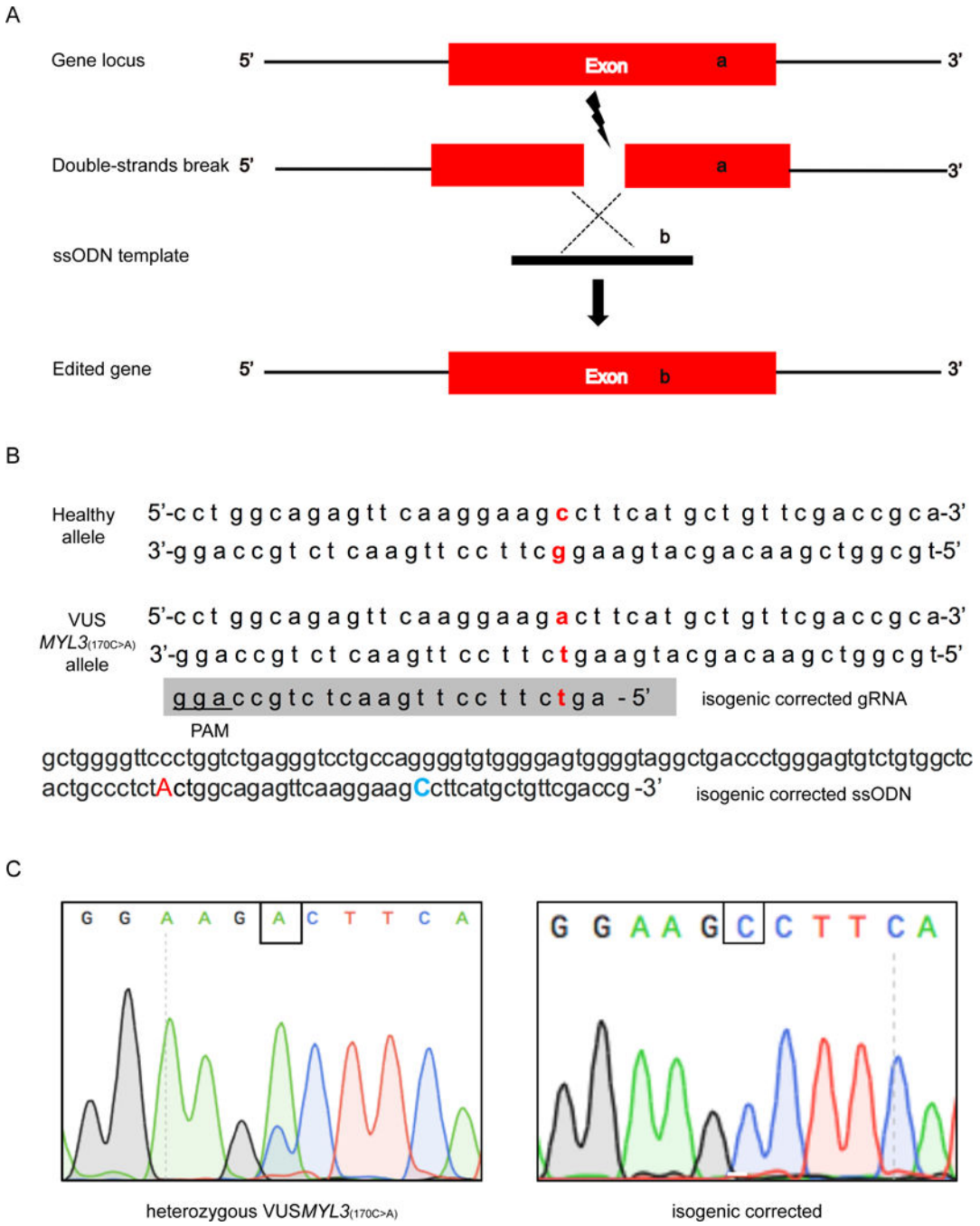

Figure 2. Genome-editing of an isogenic corrected iPSC line using CRISPR

(A) Schematic view of CRISPR/Cas9 and ssODN mediated genome editing. **(B)** Sequence of gRNA and ssODN for generating the isogenic corrected iPSC line. The blue capitalized 'C' annotates the desired Cytidine to be introduced to the VUS*MYL3*$_{(170C>A)}$ allele. The red lower-case letters display nucleotides positions of the VUS*MYL3*$_{(170C>A)}$, while the red capitalized 'A' represents a silent mutation. **(C)** Sanger sequencing confirmation of the isogenic corrected iPSC line (clone 1). Additional clones are presented in Supplemental Figure S3.

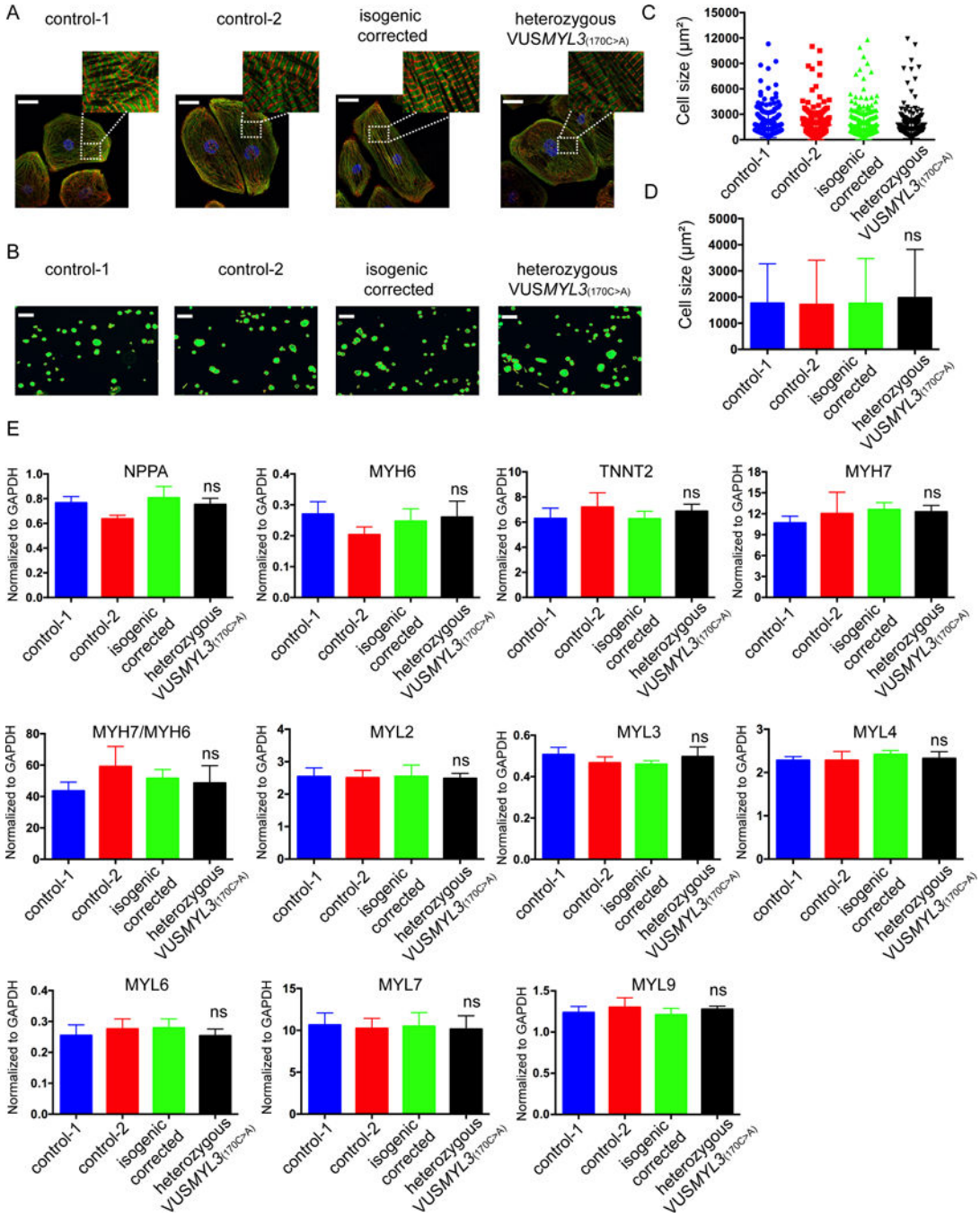

Figure 3. Cell morphology and gene expression analysis of the heterozygous VUS*MYL3*$_{(170C>A)}$ iPSC-CMs

(A) Sarcomere immunostaining analysis of iPSC-CMs differentiated from the two healthy control, isogenic corrected, and heterozygous VUS*MYL3*$_{(170C>A)}$ lines, displaying sacromeric-α-actinin (red) and troponin T (green) stainings. Scale bars represents 10 μm. **(B)** A schematic representation of cell size measurements using Phalloidin. Scale bars represents 150 μm. (**C)** Distribution of iPSC-CMs size. **(D)** iPSC-CMs size statistical analysis (n≥200 cells per line). The heterozygous VUS*MYL3*$_{(170C>A)}$-iPSC-CMs revealed

no significant difference (ns) in average cell area compared with the tested iPSC-CM lines (healthy controls-1, healthy control-2 and isogenic corrected control), **(E)** Gene expression analysis of differentiated iPSC-CMs at day 45-50 dpd. The heterozygous VUS*MYL3*$_{(170C>A)}$-iPSC-CMs revealed no significant difference in gene expression compared with the aforementioned tested iPSC-CM lines.

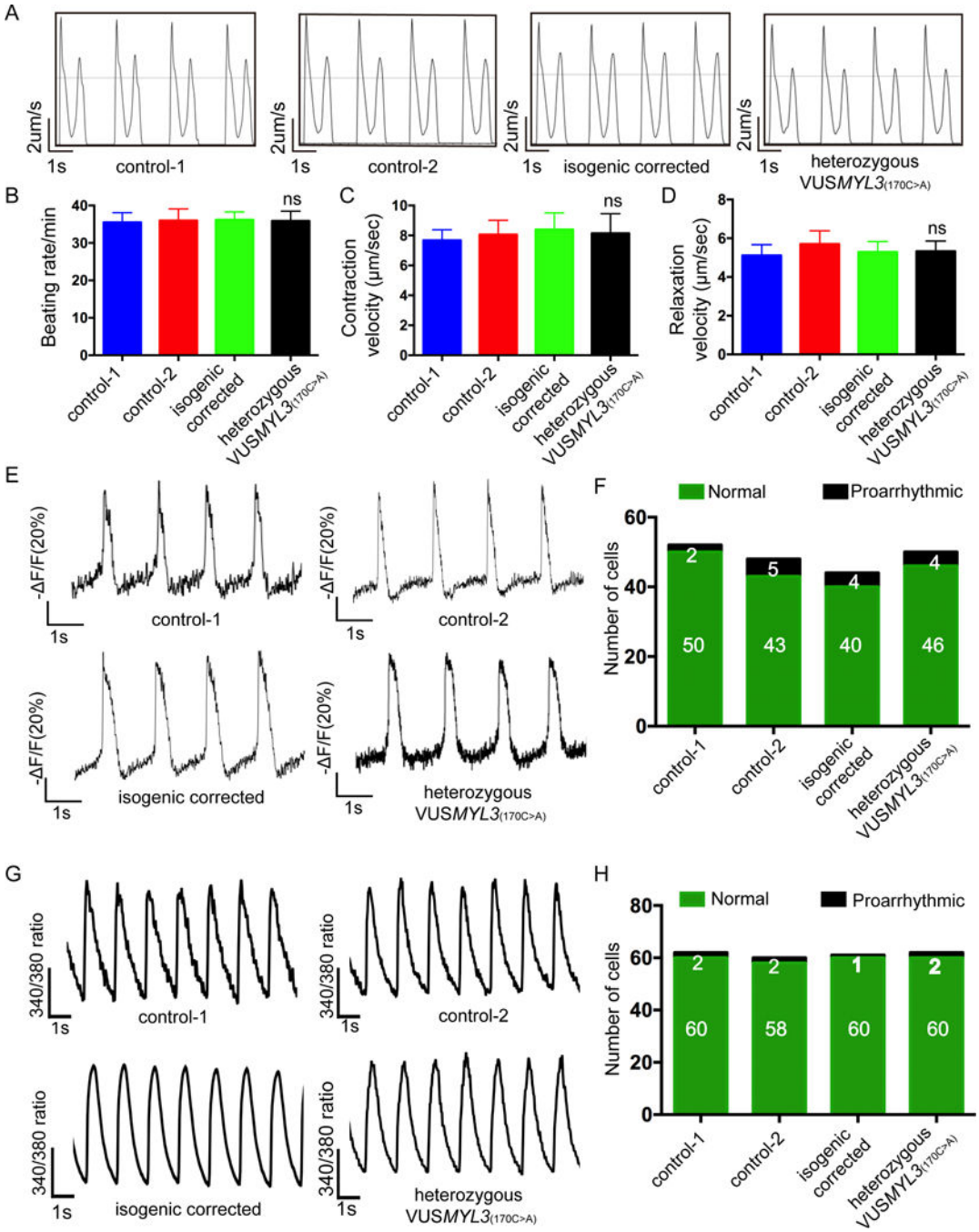

Figure 4. Comprehensive functional analysis of the heterozygous VUS*MYL3*$_{(170C>A)}$ iPSC-CMs

(A) Representative contractility traces of iPSC-CMs from the two healthy control, isogenic corrected, and the heterozygous VUS*MYL3*$_{(170C>A)}$ lines. **(B-D)** Beating rate, contraction velocity, and relaxation velocity, respectively. The heterozygous VUS*MYL3*$_{(170C>A)}$-iPSC-CMs revealed no significant difference (ns) in beating rate, contraction velocity, and relaxation velocity, respectively, compared with the aforementioned tested iPSC-CM lines. **(E)** Representative action potential traces. **(F)** Number of iPSC-CMs displaying

proarrhythmic activity. (**G)** Representative Ca^{2+} transients. (**H)** Number of iPSC-CMs showing proarrhythmic calcium transients.

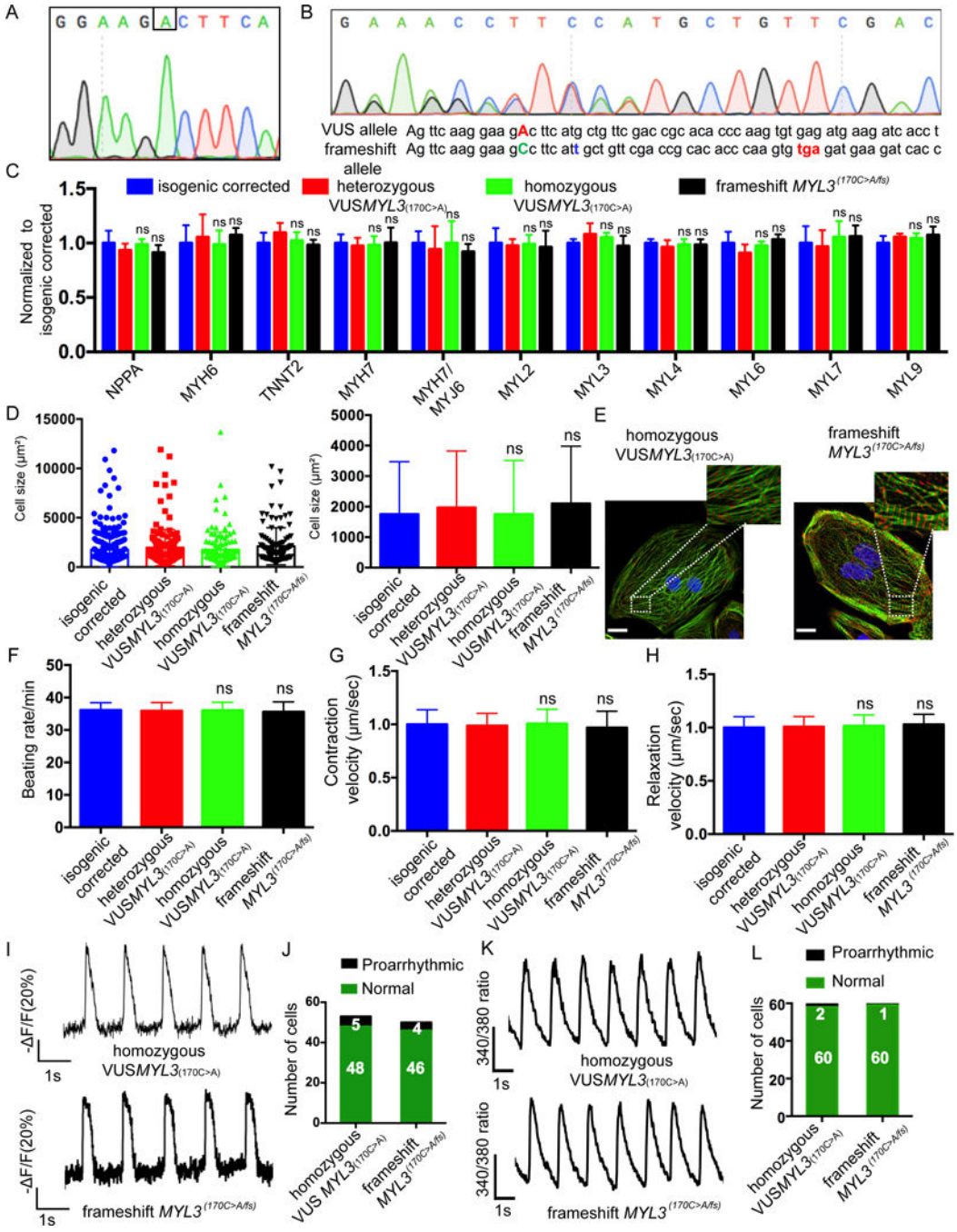

Figure 5. Comprehensive assays for assessing the homozygous VUS*MYL3*$_{(170C>A)}$ and the heterozygous frameshift mutation *MYL3*$^{(170C>A/fs)}$ iPSC-CMs

(A) Sanger sequencing confirmation of the isogenic homozygous VUS*MYL3*$_{(170C>A)}$ iPSC (clone1). Additional clones are presented in Supplemental Figure S6. **(B)** Sanger sequencing confirmation of the isogenic heterozygous frameshift mutation *MYL3*$^{(170C>A/fs)}$-iPSC (clone1). Additional clones are presented in Supplemental Figure S6. The red capitalized 'A' represents the VUS*MYL3*$_{(170C>A)}$. The blue lower-case 't' represents non-homologous end joining (NHEJ)-mediated 1bp insertion. The red lower-case letters (tga) display the

premature stop codon. **(C)** Gene expression analysis. The homozygous VUS*MYL3*$_{(170C>A)}$-iPSC-CMs and the frameshift mutation *MYL3*$^{(170C>A/fs)}$-iPSC-CMs revealed no significant difference in gene expression compared with the isogenic corrected and the heterozygous VUS*MYL3*$_{(170C>A)}$ iPSC-CMs. **(D)** Cell size assessment (n≥200 cells per line). The homozygous VUS*MYL3*$_{(170C>A)}$-iPSC-CMs and frameshift mutation *MYL3*$^{(170C>A/fs)}$-iPSC-CMs revealed no significant difference (ns) in cell size distribution (left panel) and average cell area (right panel) compared with isogenic corrected and heterozygous VUS*MYL3*$_{(170C>A)}$. **(E)** Sarcomere immunostaining analysis displaying sacromeric-α-Actinin (red) and troponin T (green) stainings. Scale bars represents 10 μm. **(F-H)** Beating rate, contraction velocity, and relaxation velocity analysis, respectively. The homozygous VUS*MYL3*$_{(170C>A)}$ and frameshift mutation *MYL3*$^{(170C>A/fs)}$-iPSC-CMs revealed no significant difference in beating rate, contraction velocity, and relaxation velocity, respectively, compared with isogenic corrected and heterozygous VUS*MYL3*$_{(170C>A)}$. **(I)** Representative action potential traces. **(J)** Number of iPSC-CMs displaying proarrhythmic activity. **(K)** Representative calcium transients. **(L)** Number of iPSC-CMs showing proarrhythmic calcium transients.

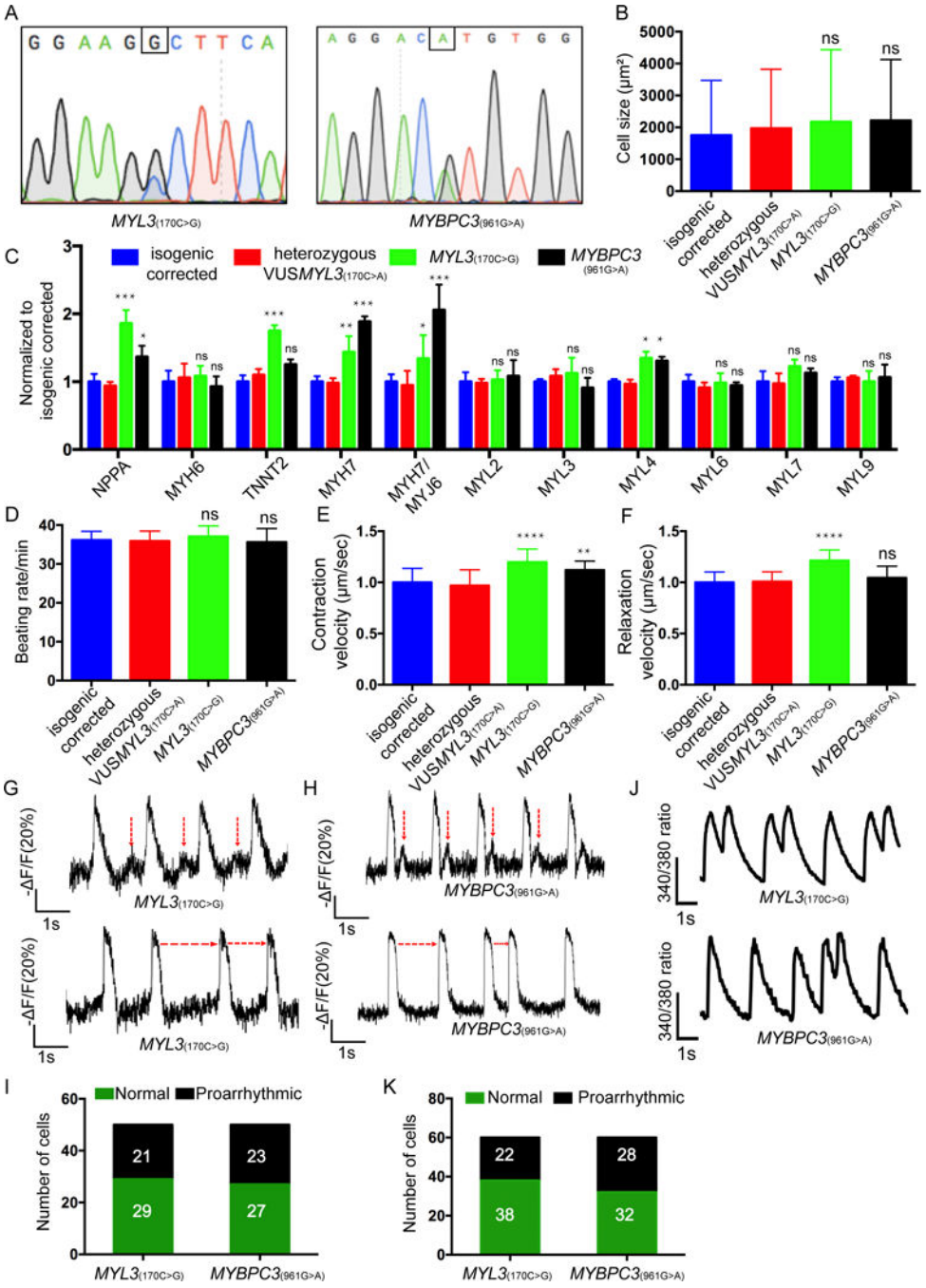

Figure 6. Comprehensive assays for assessing the *MYL3*$_{(170C>G)}$ and *MYBPC3*$_{(961G>A)}$ iPSC-CMs

(A) Sanger sequencing confirmation of the isogenic *MYL3*$_{(170C>G)}$ clone1,(Additional clones are presented in Supplemental Figure S8) and *MYBPC3*$_{(961G>A)}$ iPSC line. **(B)** Cell size assessment (n≥200 cells per line) displayed as mean ± SD. The *MYL3*$_{(170C>G)}$ and *MYBPC3*$_{(961G>A)}$ iPSC-CMs revealed no significant difference (ns) in average cell area compared with isogenic corrected and heterozygous VUS*MYL3*$_{(170C>A)}$. **(C)** HCM-related gene expression analysis. The *MYL3*$_{(170C>G)}$ and *MYBPC3*$_{(961G>A)}$ iPSC-CMs revealed no

significant difference in gene expression compared with the isogenic corrected and the heterozygous VUS*MYL3*$_{(170C>A)}$ iPSC-CM lines. **(D-F)** Beating rate, contraction velocity, and relaxation velocity, respectively. The *MYL3*$_{(170C>G)}$ and *MYBPC3*$_{(961G>A)}$ iPSC-CMs revealed no significant difference in beating rate, contraction velocity, and relaxation velocity, respectively, compared with isogenic corrected and heterozygous VUS*MYL3*$_{(170C>A)}$. **(G-H)** Representative action potentials traces displaying DADs (highlighted by red vertical arrows) and varying inter-beats intervals (indicated by red horizontal arrows) recorded from *MYL3*$_{(170C>G)}$ and *MYBPC3*$_{(961G>A)}$ iPSC-CMs, respectively. **(I)** Number of *MYL3*$_{(170C>G)}$ and *MYBPC3*$_{(961G>A)}$ iPSC-CMs displaying proarrythmic activity **(J)** Representative Ca^{2+} transients displaying DADs. **(K)** Number of *MYL3*$_{(170C>G)}$ and *MYBPC3*$_{(961G>A)}$ iPSC-CMs depicting proarrhythmic calcium transients. *$p < 0.1$, ** $p < 0.01$, *** $p < 0.001$, **** $p < 0.0001$, compared with isogenic corrected and heterozygous VUS*MYL3*$_{(170C>A)}$ lines.

Table 1

ClinVar report for VUS *MYL3*(170C>A)

Clinical significance (Last evaluated)	Collection method	Condition(s) (Mode of inheritance)	Submitter – Study name	Description
Uncertain significance (Aug 29, 2013)	clinical testing	not specified [MedGen]	Laboratory for Molecular Medicine, Partners HealthCare Personalized Medicine	None
Uncertain significance (May 18, 2017)	clinical testing	not specified [MedGen]	GeneDx	Based on the currently available information, it is unclear whether this variant is a pathogenic variant or a rare benign variant
Uncertain significance (Nov 30, 2015)	clinical testing	Cardiomyopathy [MedGen | Orphane]	Division of Genomic Diagnostics, The Children's Hospital of Philadelphia	None
Likely pathogenic (Oct 31, 2016)	clinical testing	not provided [MedGen]	Praxis fuer Humangenetik Tuebingen	Ala57Asp variant may be pathogenic, additional studies are needed to fully assess its clinical significance
Uncertain significance (Jul 7, 2014)	clinical testing	Primary familial hypertrophic cardiomyopathy [MedGen | Orphanet|OMIM]	Blueprint Genetics	Found together with likely pathogenic MYBPC3 (NM_000256.3:c.3800G>A)

Table 2

Echocardiography results for individuals with *MYL3* c.170C>A or *MYBPC3* c. 961G>A.

	***MYL3* c.170C>A Individual I. 2**	***MYL3* c.170C>A Individual II.2**	***MYL3* c.170C>A Individual II.1**	***MYL3* c.170C>A Individual III.2**	***MYBPC3* c.961G>A Patient**
LVID (cm)	4.5	4.7	5.4	4.4	4.5
Septal WT (cm)	0.85	0.82	0.92	0.67	1.8
Posterior WT (cm)	0.87	0.88	0.85	0.74	0.92
Relative WT	0.38	0.36	0.33	0.32	0.41
LV mass index (g/m^2)	75	66	84	65	151
LVEF (%)	70	68	61	67	48.7
E (cm/s)	69	62	51	90	58.7
E/A	1.3	0.9	1	2	1.4
e' average (cm/s)	6.5	7.0	10	13	7.1
E/e'	11	8.9	5.1	6.9	8.5
LAV index (mL/m^2)	28	23	21	24	41.2
Estimated RAP (mmHg)	3	3	3	3	10
Septal curvature	Normal	Normal	Normal	Normal	Reverse curvature

LVID: left ventricular diastolic diameter, WT: wall thickness, LV: left ventricular, LVEF: left ventricular ejection fraction, E: peak early diastolic transmitral flow velocities, E/A: peak early and late diastolic transmitral flow velocities ratio, E/e': peak early diastolic transmitral flow velocities and peak early diastolic mitral annular velocities ratio, LAV: left atrial volume, RAP: right atrial pressure. *MYL3* c. 170C>A individuals: I.2 70 yo mother; II.1 48 yo brother; II.2 46 proband; III.2 11 yo daughter.